Diurnal modulation of multivesicular release controls the efficiency of information transmission at a sensory synapse

José Moya-Díaz, Ben James, Federico Esposti, Jamie Johnston and Leon Lagnado*

Sussex Neuroscience, School of Life Sciences, University of Sussex,
Brighton BN1 9QG, UK

*Corresponding author: l.lagnado@sussex.ac.uk

Summary

Neuromodulators adjust sensory circuits to changes in the external world or the animal's internal state and synapses are key control sites for such plasticity. Less clear is how neuromodulation alters the amount of information transmitted through the circuit. We investigated this question in the context of the diurnal regulation of visual processing in zebrafish, focusing on synapses of retinal bipolar cells. We demonstrate that contrast-sensitivity peaks in the afternoon accompanied by an average four-fold increase in the Shannon information transmitted at individual active zones. This increase reflects higher synaptic gain, lower spontaneous "noise" and reduced variability of evoked responses. Simultaneously, an increase in the probability of multivesicular events with larger information content increases the efficiency of transmission (bits per vesicle) by factors of 2-3. This study demonstrates how the potentiation of multivesicular release by neuromodulators can increase the synaptic transfer of information and the efficiency of the vesicle code.

Introduction

It has long been understood that the flow of signals through neural circuits is adjusted by neuromodulators[1]. Less clear is how these alter the amount of information that is transmitted through the circuit. Here we investigate this question in the context of visual processing in the retina.

The retina is highly plastic: the input-output relation can adapt within seconds to the recent history of the visual stimulus[2,3] or, on longer time-scales, to changes in the animal's internal state[4,5]. In diurnal animals, for instance, retinal sensitivity to light is regulated both by the daily light-dark cycle and by intrinsic circadian clocks[6-8] . Key to these adjustments is dopamine, a neuromodulator which is released from amacrine cells in a circadian cycle, varying from a minimum at night, increasing during the day and peaking before dusk[6,9]. But the average luminance of a visual scene is not the variable driving most behaviours related to vision: navigation, finding food and avoiding predators all depend on detection of fast modulations in light intensity. We therefore investigated the diurnal control of temporal contrast processing, focusing on the visual signal transmitted by glutamatergic synapses of bipolar cells.

Bipolar cells are the bridge between the photoreceptors and ganglion cells that deliver the results of retinal processing to downstream circuits. Their synaptic compartments are an important control point for transformations of the visual signal[10] and contribute to a number of processing tasks, from adaptive gain control to temporal filtering and the coding of motion, colour, orientation and direction[3,11-13]. Bipolar cells are similar to other sensory neurons, such as photoreceptors, sensory hair cells and electroreceptors, in transmitting information through ribbon synapses containing specialized structures that supply vesicles to the active zone[14]. These sensory synapses do not always operate as Poisson machines in which vesicles are released independently but also signal through multivesicular release (MVR), where the fusion of two or more vesicles is co-ordinated as a single synaptic event[15-17]. The importance of MVR at a number of sites in the brain is now recognized and it has been suggested

that it might contribute to more complex strategies for transmitting information than modulation of a rate code[18-20].

It is difficult to use Shannon's information theory to measure the amount of information transmitted at a synapse because the experimenter needs to observe the symbols conveying the message while also observing or controlling the sensory input[21,22]. This has recently been achieved by multiphoton imaging of the glutamate reporter iGluSnFR[23] in bipolar cells of larval zebrafish, where it is found that the visual message transmitted from an active zone does not use a simple binary code but is instead composed of a number of symbols, composed of one, two, three or more vesicles released as one event[17]. Here we demonstrate that this strategy of coding by amplitude as well as rate is under diurnal control. Synaptic responses to temporal contrast reach a maximum in the afternoon and are accompanied by a four-fold increase in the Shannon information transmitted at each active zone compared to the morning. Dopamine contributes to this increase in information transfer by reducing several aspects of synaptic “noise” and by increasing the probability of multivesicular events with larger information content, which in turn increases the efficiency of transmission quantified as bits per vesicle.

Results

Differential regulation of luminance-sensitivity and contrast-sensitivity

To investigate the diurnal modulation of visual processing in larval zebrafish we began by imaging synaptic activity in bipolar cells with SyGCaMP2[24] (Fig. 1A). When animals were placed on a cycle of 14 hours light and 10 hours dark, no significant synaptic responses could be detected at *Zeitgeber* times 18-0 hours, consistent with previous observations that larvae are blind at subjective night[25]. Visual sensitivity began to recover within 20 mins of light onset, after which responses gradually

84 increased in amplitude (Fig. S1A and Fig. 1B). Plotting the irradiance-response
85 functions (Fig. 1C) allowed the luminance sensitivity to be quantified as the inverse of
86 the irradiance generating a half-maximal response ($1/I_{1/2}$). Over the course of the day,
87 luminance-sensitivity increased gradually over a range greater than 200-fold (Fig. 1D).
88 As in other species, this increase could be explained largely by actions of D2
89 dopamine receptors because injection of the antagonist sulpiride (~2 μM) reduced
90 luminance-sensitivity in the afternoon to levels measured in the morning[6] (Fig. S1).

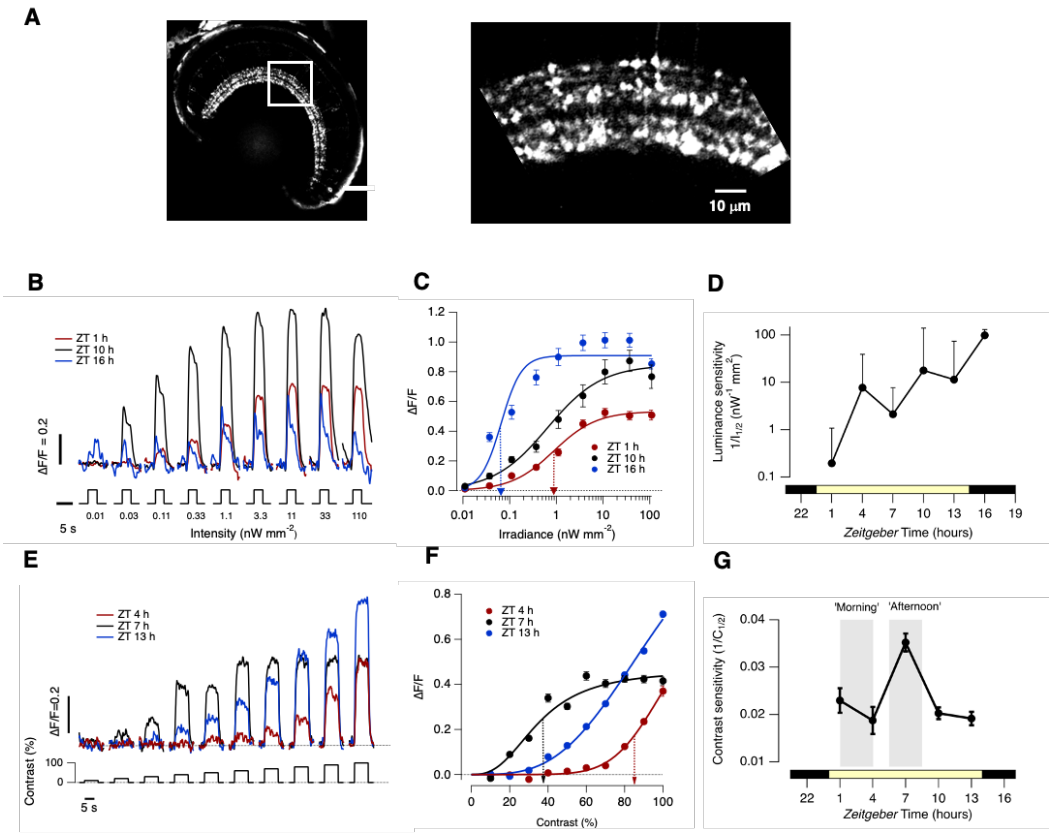

91

92 **Figure 1: Differential regulation of luminance-sensitivity and contrast-sensitivity**

93 **A.** Left: Retina of a Ribeye::SyGCaMP2 fish with box over the IPL. Right: expansion of the boxed region of
94 showing terminals of bipolar cells. **B.** Averaged responses from ON terminals to light steps of different
95 irradiance measured at *Zeitgeber* time 1, 10 and 16 hours. Note large variations in amplitude and
96 kinetics. Each light step was of 3 s (*n* = 535 terminals from 10 fish). **C.** Peak response as a function of
97 irradiance for ON terminals in B. The smooth lines are Hill functions of the form $R = R_{max}*(I^h/(I^h + I_{1/2}^h))$,
98 where R is the peak response, I is the irradiance, h is the Hill coefficient and $I_{1/2}$ is the irradiance
99 generating the half-maximal response. At ZT = 16 hrs: R_{max} = 0.91 ± 0.04; h = 2.0 ± 0.2; $I_{1/2}$ = 0.066 ±
100 0.02 nW/mm^2 (dashed blue arrow). At ZT = 10 hrs: R_{max} = 0.85 ± 0.06; h = 0.8 ± 0.1; $I_{1/2}$ = 0.65 ± 0.18
101 nW/mm^2. At ZT = 1 hrs: R_{max} = 0.853 ± 0.02; h = 0.9 ± 0.2; $I_{1/2}$ = 0.88 ± 0.18 nW/mm^2 (red arrow). **D.**
102 Variations in luminance sensitivity as a function of *Zeitgeber* time averaged across both ON and OFF

terminals (n=535 and 335, respectively). The lower bar shows the timing of the light-dark cycle. **E.** Averaged responses to stimuli of different contrasts measured at *Zeitgeber* time 4, 7 and 13 hrs. **F.** Peak response amplitude as a function of contrast for terminals shown in E. The smooth lines are Hill functions used to interpolate values of $C_{1/2}$, the contrast generating the half-maximal response. Note the diurnal variations. At ZT = 4 hrs: $C_{1/2}$ = 86 ± 2% (dashed red arrow); h = 7.0 ± 1.2. At ZT = 7 hrs: $C_{1/2}$ = 35 ± 2% (dashed black arrow); h = 2.7 ± 0.2. At ZT = 13 hrs: $C_{1/2}$ = 72 ± 2%; h = 3.3 ± 0.2. **G.** Variations in contrast-sensitivity as a function of *Zeitgeber* time averaged across ON and OFF terminals. Note the peak around ZT = 7 hours which is not mirrored in the diurnal variation in luminance sensitivity (D). The grey bars show the periods described as "morning" and "afternoon". All error bars show ± 1 SD.

The detection of modulations in light intensity (contrast) was also under diurnal control, but with a distinctive time-course (Fig. 1E-G; 5 Hz full-field stimuli). At ZT = 4 hours, temporal contrasts below 50% were barely detected and the half-maximal response ($C_{1/2}$) was generated by a contrast of 86 ± 2 % (Figs. 1E and F). But at ZT = 7 hours $C_{1/2}$ it fell to 35 ± 2 % with responses saturated above 50%. When contrast sensitivity ($1/C_{1/2}$) was mapped during the course of the day it was relatively constant at ZT 1-5 hours and ZT 9-14 hours but increased to levels ~2.4-fold higher around ZT = 7 hours (Fig. 1G). Notably, this peak in the contrast sensitivity of the retinal circuit occurred at a similar *Zeitgeber* time as the maximum contrast sensitivity measured behaviourally using the optokinetic reflex[8,26]. A qualitatively similar increase in contrast sensitivity was also observed at the retinal output projecting to the optic tectum (Fig. S2).

Diurnal regulation of contrast gain

To measure transmission of the visual signal in terms of its elementary units – synaptic vesicles - we expressed the reporter iGluSnFR[23] sparsely in bipolar cells (Fig. 2A). Wiener deconvolution of iGluSnFR signals allowed us to count released vesicles (see Methods and Fig. S3; detailed evidence that these methods allow signals to be isolated from individual active zones vesicles has been described[17]). Synaptic function was compared over a two-hour period beginning 1 hour after light onset ("morning") with a two-hour period beginning 6 hours later ("afternoon"; Fig. 1G).

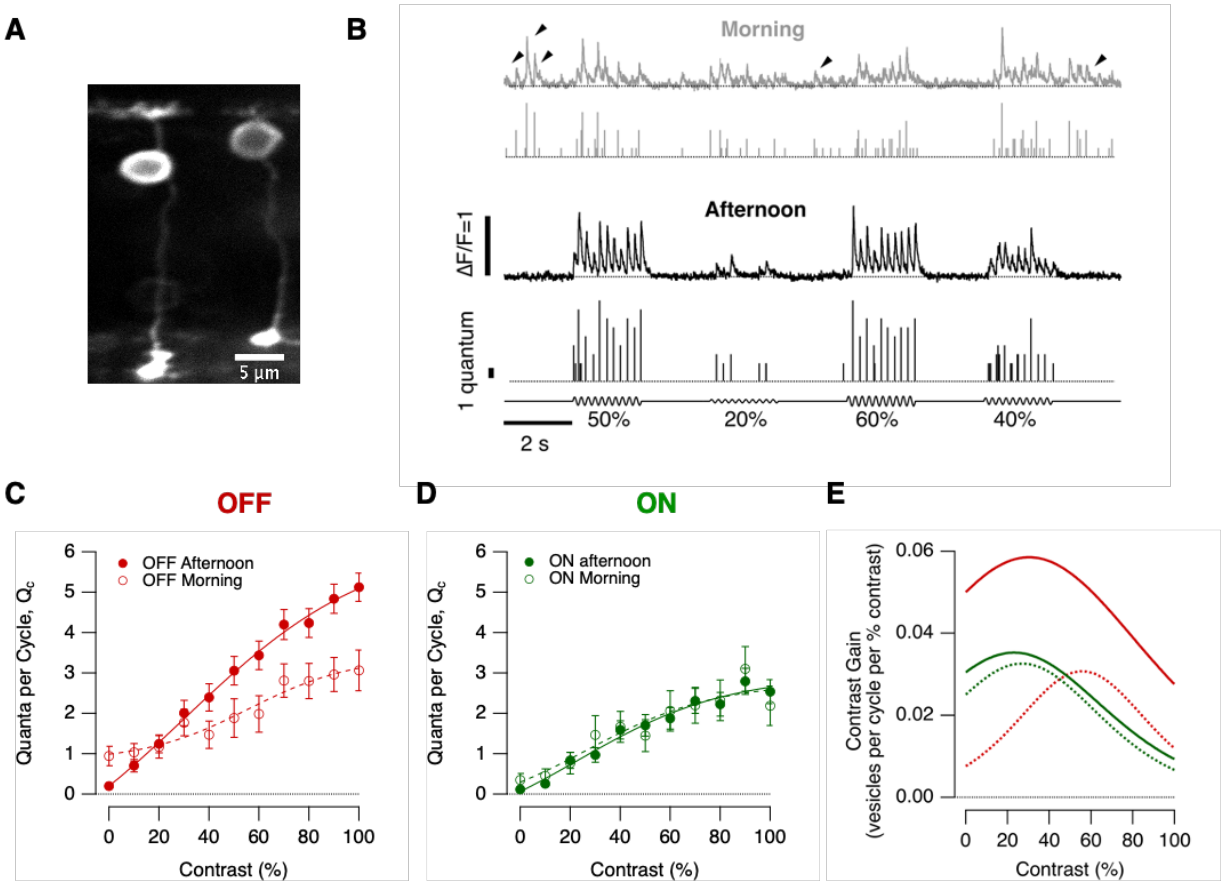

Figure 2. Diurnal modulation of synaptic gain

A. Multiphoton section through the eye of a zebrafish larva (7 dpf) expressing iGluSnFR in a subset of bipolar cells. **B**. Examples of iGluSnFR signals from an individual OFF synapse elicited using a stimulus of variable contrast modulated at 5 Hz (0-100%, full field, sine wave) in the morning (ZT 1-3 hours, grey) and afternoon (ZT 6-9 hours, black). Note the high levels of spontaneous activity in the morning (black arrowheads). In each case the top trace shows the iGluSnFR signal and the lower trace the estimated number of quanta composing each event (Q_e). **C.** Average contrast-response functions in OFF bipolar cell synapses in the morning (open circles; n = 20 synapses) and afternoon (closed; n = 59), where the response (*R*) was quantified as the average of quanta per cycle (Q_c). The smooth lines are fits of a sigmoid used for smoothing. Note the differences in the shape of the contrast-response functions and in the levels of spontaneous activity (zero contrast). **D.** Average contrast-response functions in ON bipolar cell synapses in the morning (open circles; n = 12 synapses) and afternoon (closed; n = 31). There was no significant difference in in the morning relative to afternoon (Chi-square test, p = 0.9999). **E.** The contrast gain calculated as the derivative of the fits to the contrast-response functions in C and D. Note that the maximum contrast discrimination is increased by a factor of 2x in the OFF channel during the afternoon.

155 Examples of glutamate transients at an individual OFF active zone are shown in
156 Fig. 2B. Across a range of contrasts, responses were, on average, larger in the
157 afternoon. We began by measuring the contrast-response function (CRF) simply as
158 the average number of vesicles released per cycle of a 5 Hz stimulus, choosing this
159 frequency because the integration time of a bipolar cell is ~200 ms[27]. There was little
160 diurnal modulation of the CRF measured at ON synapses but in the OFF channel the
161 maximum rate of release measured at 100% contrast increased from 15.25 ± 2.5
162 vesicles/s in the morning to 25.5 ± 1.5 vesicles/s in the afternoon (Fig. 2C and D).
163 This increase in synaptic gain was accompanied by an increase in contrast sensitivity,
164 and the combined effects were assessed as the derivative of the CRF ("contrast gain";
165 Fig. 2E). Contrasts in natural visual scenes rarely exceed 40%[12] and in the morning
166 this range was signalled best through the ON channel. But in the afternoon the OFF
167 channel became dominant, with contrast gains increasing by factors of 2-6.
168
169 **Dopamine regulates contrast gain**
170 To test whether dopamine contributes to diurnal changes in contrast sensitivity we
171 injected agonists or antagonists of dopamine receptors directly into the eye. Fig. 3A
172 shows examples of the output from a synapse imaged in the afternoon, before and
173 after injection of the D1 receptor antagonist SCH 23390 (estimated final concentration
174 of 0.1 μM). Counteracting the actions of endogenous dopamine reduced the average
175 rate of vesicle release and shifted the CRF such that the maximum contrast gain was
176 achieved at higher contrasts (black points in Fig. 3B and C). Conversely, increasing
177 activation of D1 receptors in the morning by injection of the agonist ADTN (~0.2 μM)
178 increased response gain.

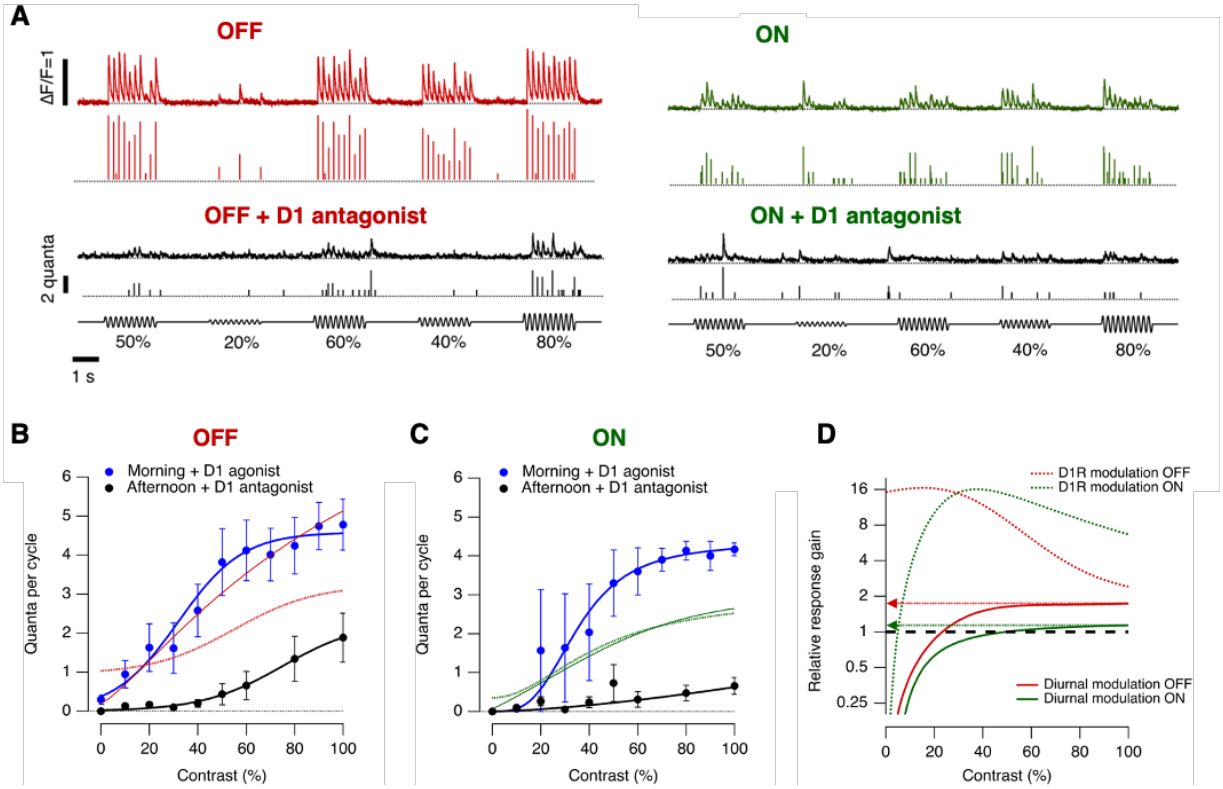

Figure 3. Diurnal changes in dopamine levels modulate synaptic transmission.
A.Examples of iGluSnFR signals recorded in the afternoon from an individual OFF (red trace) and ON (green trace) synapses elicited using a stimulus of variable contrast before and after intravitreal injection of the D1 antagonist, SCH 23390 (black traces; 5 Hz modulation). Note that SCH 23390 abolished synaptic responses at lower contrasts in ON and OFF synapses. In each case the top trace shows the iGluSnFR signal and the lower trace the estimated Q_e. **B.** Average contrast-response functions in OFF bipolar cell synapses after administration of D1 antagonist (black dots) in the afternoon and after administration of the D1 agonist ADTN in the morning (blue dots). Each point shows the mean ± s.e.m. (SCH 23390, n =12 synapses; ADTN, n = 12 synapses). Control responses observed in the morning and afternoon are superimposed in the graph (red lines, see Fig. 2C) **C.** Average contrast-response functions in ON bipolar cell synapses in three conditions: afternoon (green dots), after intravitreal injection of D1 antagonist in the afternoon (black dots) and ADTN in the morning (blue dots). Each point shows the mean ± s.e.m. (SCH 23390, n =7 synapses; ADTN, n = 5 synapses). Control responses observed in the morning and afternoon are superimposed to the graph (green lines, see Fig. 2D). **D**. Relative response gain by diurnal modulation and after manipulation of dopaminergic signalling (dashed lines). Note that diurnal modulation of synaptic gain is higher in OFF synapses, whereas dopamine modulates the dynamic range by ~16 fold-change in ON and OFF synapses.

The dynamic range over which D1 receptors adjusted synaptic gain was calculated as the ratio of the CRFs in the presence of the agonist and antagonist: in both ON and OFF channels the maximum modulation was ~16-fold, occurring at

contrasts of 20-40% (Fig. 3D). But diurnal modulation of gain was narrower than this potential range: 1.7-fold in OFF synapses and 1.1-fold in ON. This difference reflected, at least in part, a gain in the morning that was at least 5-fold higher than that measured with D1R receptors blocked, consistent with dopamine levels that were already high enough to potentiate synaptic transmission (Fig. 3B and C). These manipulations of retinal dopamine receptors caused qualitatively similar changes in the signals that ganglion cells transmit to the optic tectum (Fig. S2).

Modulation of synaptic noise and variability

How does diurnal modulation of contrast processing affect the information transmitted to ganglion cells? In the framework of information theory[21], an increase in synaptic gain will tend to reduce uncertainty (and therefore increase information) by causing a larger change in the number of vesicles released when contrast changes. But information is degraded by "noise" that causes responses to vary when the same stimulus is repeated and synapses are a major source of such variability within neural circuits[28,29]. One cause of synaptic noise is the stochasticity of the presynaptic processes that control the fusion of vesicles[18] and this was a prominent feature of the output from synapses of bipolar cells (Figs. 2B). We distinguished four aspects of synaptic variability and investigated the diurnal modulation of each; i) spontaneous vesicle release (Fig. 4), ii) variability in the number of vesicles released by a stimulus (Fig. 5), iii) variability in the timing of release events i.e how tightly they are time-locked to the stimulus (Fig. 6) and iv) modulation of multivesicular release (Fig. 7). Finally, we calculated how these different aspects of synaptic "noise" combined with changes in contrast gain (Fig. 3) to alter the amount of visual information transferred from individual active zones (Fig. 8).

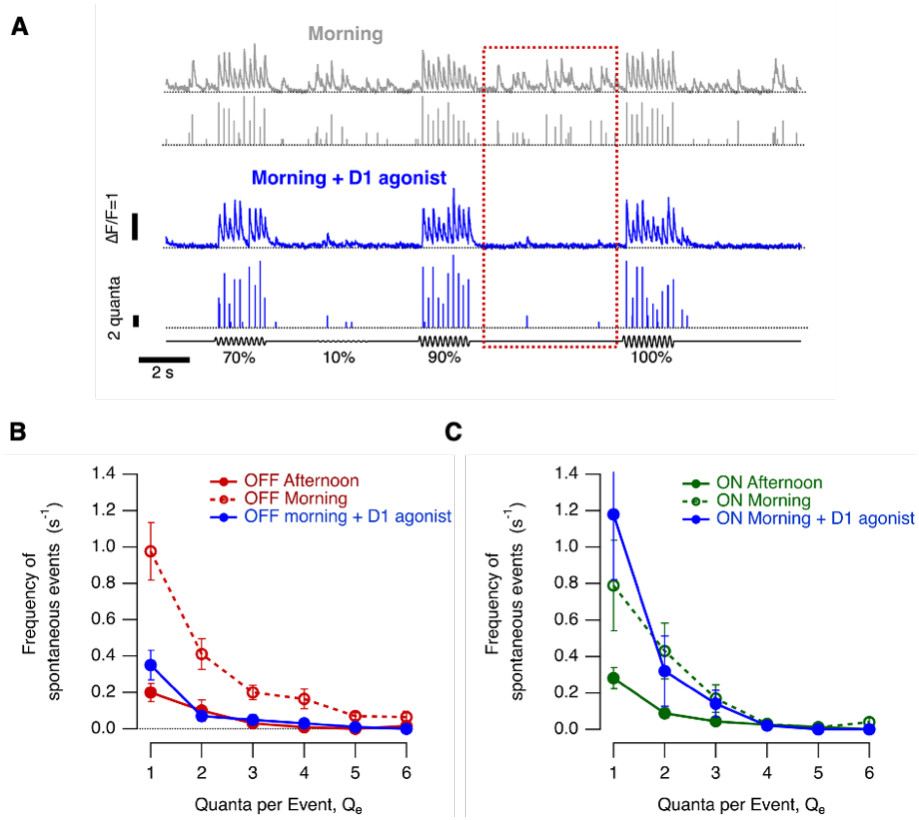

Figure 4. Diurnal modulation of spontaneous synaptic noise

A. *Top:* Example of iGluSnFR signals from an individual OFF synapse elicited using a stimulus of variable contrast in the morning (0-100%, 5 Hz modulation). In this example, note the high levels of spontaneous activity that were quantified as the responses elicited at zero contrast (red dashed box) . *Bottom.* Examples of iGluSnFR signals from the same OFF synapse after intravitreal injection of ADTN. Note the increase in amplitude and frequency of events and the reduction of spontaneous activity. In each case the top trace shows the iGluSnFR signal and the lower trace the estimated Q_e. **B.** Quantification of spontaneous events composed by different Q_e in OFF synapses in the morning, morning + ADTN and afternoon (OFF morning, n = 20 synapses; OFF morning + ADTN= 12 synapses; OFF afternoon, n=24 synapses). Note the suppression of spontaneous events in OFF synapses after intravitreal injection of ADTN in the morning. **C.** Quantification of spontaneous events composed by different Q_e in ON synapses in the Morning, Morning + ADTN and Afternoon (ON Morning = 12 synapses; ON Morning + ADTN = 5 synapses; ON Afternoon, n =17 synapses). Note that spontaneous activity levels were not dramatically altered after administration of ADTN.

i) Spontaneous release

Increases in synaptic gain were accompanied by a *decrease* in the spontaneous release of vesicles in the absence of a visual stimulus. In the morning, spontaneous release occurred at relatively high rates (Fig. 4A) composed of both univesicular and

248 multivesicular events (Fig. 4B and C). Integrating across events of all amplitudes, the
249 average rate of spontaneous release in OFF synapses was 22.5 ± 12.5 vesicles s^{-1} in
250 the morning, falling to 5 ± 1 vesicles s^{-1} in the afternoon (Fig. 4B). In ON synapses
251 these values were 9 ± 4 vesicles s^{-1} and 2.5 ± 1 vesicles s^{-1} (Fig. 4C). In both channels,
252 therefore, spontaneous noise was ~4 times lower in the afternoon compared to the
253 morning. Increased activation of D1 receptors suppressed spontaneous release in the
254 morning to levels close to those measured in the afternoon, but only in OFF synapses
255 (Fig. 4B and C).
256
257 ***ii) Variability in stimulus-evoked responses.***
258 When recording neural responses as spikes, the Fano factor is measured as the ratio of
259 the variance-to-mean of spikes counted in a fixed time-window after a repeated
260 stimulus[30,31]. We calculated the Fano factor of a synapse by counting the number of
261 vesicles released over each cycle of a sinusoidal stimulus (Fig. 5A). In the morning, F
262 was ~2.6 in both ON and OFF synapses when averaged over a range of contrasts, falling
263 to ~1.6 in the afternoon (both significant at $p < 0.002$, KS test; Fig. 5B-C). The increase
264 in contrast gain and sensitivity in the afternoon (Fig. 2C-D) was therefore also associated
265 with increased reliability of bipolar cell synapses. Notably, the variability of synaptic output
266 was higher than expected for a Poisson process, for which the Fano factor is one. The
267 spike responses of post-synaptic RGCs are less variable, with a Fano factor as low as 0.3
268 at higher contrasts[30], likely reflecting the integration of signals from multiple synaptic
269 inputs. Activation of D1 receptors in the morning improved the reliability of synaptic
270 responses to levels similar to those measured in the afternoon (Figs. 5D and E).
271
272

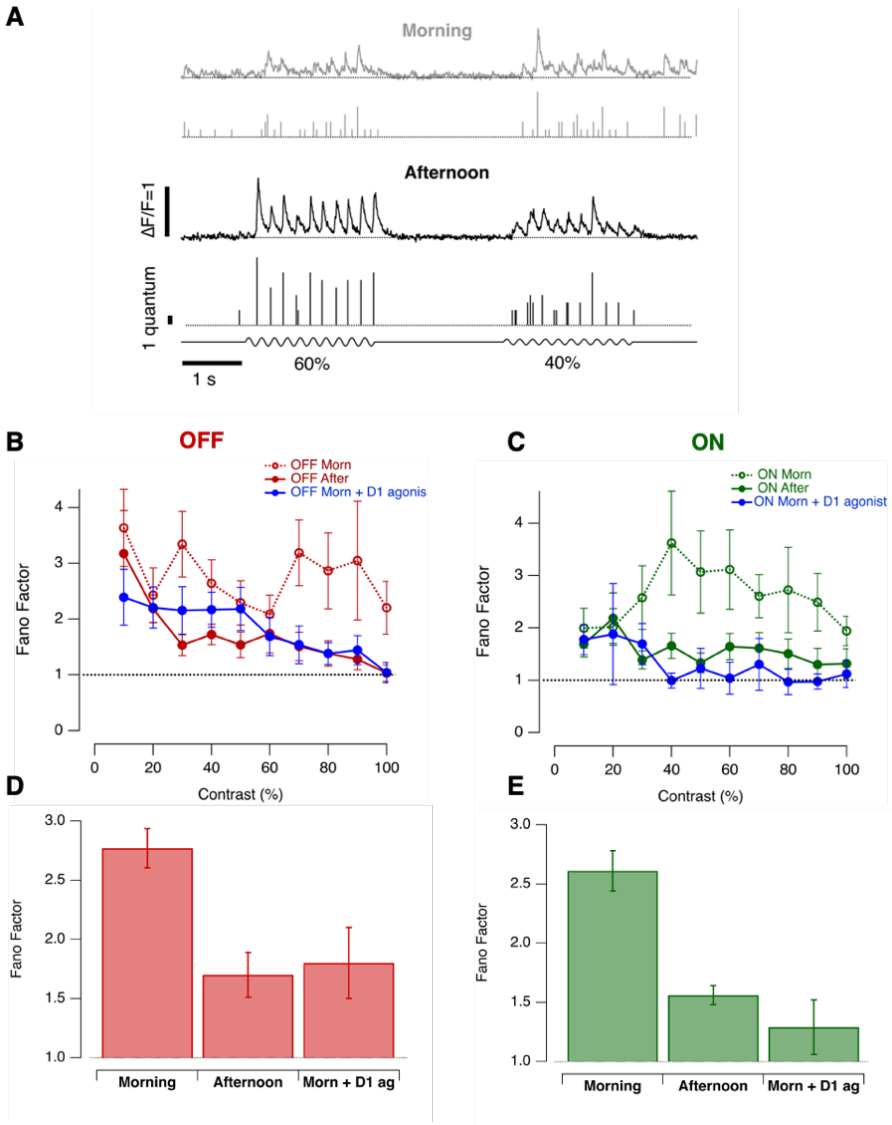

Figure 5. Diurnal changes in the variability of stimulus-evoked responses

A. Examples of iGluSnFR signals from individual OFF synapses in the morning and afternoon. Responses elicited by stimuli of 60% and 40% contrast varied from cycle to cycle of the 5 Hz stimulus. In each case the top trace shows the iGluSnFR signal and the lower trace the estimated Q_e **B.** Variability in the response of OFF synapses calculated as the Fano factor, where each response was quantified as the total number of vesicles released over one cycle at the contrasts shown. Comparison is made between the morning (n=18), afternoon (n=27) and the morning after injection of ADTN (n=13). **C**. As in B, but for ON synapses (n = 12, 15 and 6 synapses for respective conditions). **D.** Average Fano factor over different contrasts in OFF synapses in the three conditions described above. Overall, the average fano factor was significantly higher in the morning compared to afternoon or in the morning after injection of ADTN (t-test; $p<0.0001$). **E.** As D, but for ON synapses. Again, the average Fano factor was significantly higher in the morning (t-test; $p<0.001$).

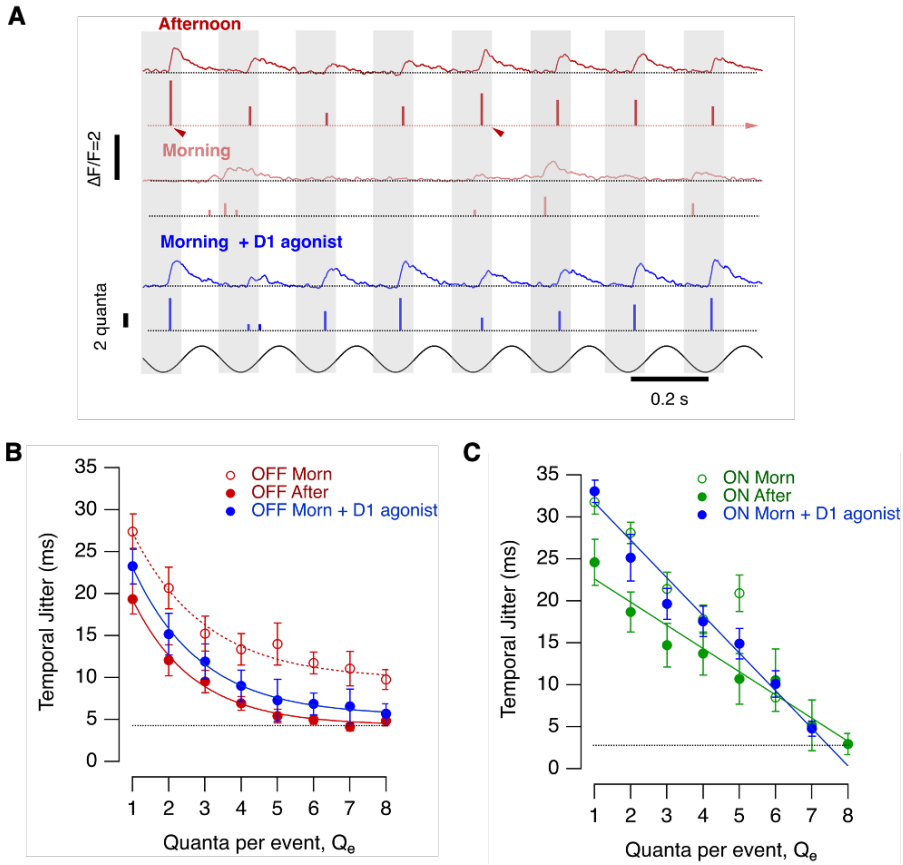

Figure 6. The temporal precision of MVR is under diurnal control in the OFF channel

A. Example recordings from two OFF synapses stimulated at 60% contrast in three conditions: afternoon (top, black trace), morning (middle, red trace) and after intravitreal injection of ADTN in the morning (bottom, blue trace). Morning and morning + ADTN synaptic responses are from the same synapse. The modulation in intensity (5 Hz, sine wave) is shown below. Arrowheads highlight events occurring at different phases of the stimulus, with less variation with events composed for 4 or more quanta in the afternoon and after administration of ADTN in the morning. In each case the top trace shows the iGluSnFR signal and the lower trace the estimated Q_e. **B.** Temporal jitter of events composed of different numbers of quanta in OFF synapses in the afternoon (red dots ; n = 24 synapses); Morning (open red dots; n = 19 synapses) and Morning + ADTN (blue dots, n = 16). Note that during the morning events composed by multiple quanta were less phase-locked to the stimuli in comparison to the afternoon. Activation of D1 receptors had a significant effect on release of multiquantal events. Events composed by 5 or more quanta jittered by ~7 ms, similar to values observed in the afternoon. The solid lines describing these relations in the three conditions are better described by a single exponential decay function of the form $y_0 + A_{exp}((-(x-x_0)/\tau)))$ with y0= 4.23 ± 1.2 and A = 27 ± 7 in the afternoon; y0= 9.77 ± 1.4 and A= 28.64 ± 5.6 in the morning and y0=5.45 ± 1.3, A = 30. ± 6.1 after activation of D1 receptor in the morning. **C.** Temporal jitter of events composed by different numbers of quanta measured in ON synapses in the afternoon (green dots; n = 14 synapses) during the (open green dots; n= 10 synapses) and during Morning + ADTN, (blue dots; n=6 =synapses). Activation of D1 receptor did not have a significant effect in the temporal precision in the ON channel. The relationship observed in the morning is better described by a straight line with a = 34.7 ± 1.5 and a slope = -3.6 ± 0.5.

309 ***iii) Temporal jitter***.

310 Retinal ganglion cells (RGCs) encode information not just in their spike count but also
311 in the timing of spikes[30,32]. Spike times can vary by just a few milliseconds and this
312 accuracy depends on the precision of excitatory inputs received from bipolar cells[33].
313 The standard deviation in timing of release events ("temporal jitter") was measured
314 relative to the phase of a 5 Hz stimulus (60% contrast; Fig. 6A) and the larger the
315 release events the more precise it was on average (Fig. 6B-C). In OFF synapses the
316 temporal jitter was 5-8 ms higher in the morning compared to the afternoon for events
317 composed of up to 8 vesicles (Fig. 6B; $p < 0.008$, Kolomogorov-Smirnov test). Diurnal
318 modulation of temporal precision was weaker in ON synapses and only significant for
319 events composed of 1-3 vesicles (Fig. 3H; t-test at each Q_e). Increasing activation of
320 D1 receptors in the morning reduced temporal jitter in events composed for multiple
321 quanta in OFF synapses ($p < 0.05$; KS test) but not ON (Fig. 6B and C; $p > 0.5$).
322 Diurnal variations in dopamine therefore modulate the temporal accuracy of vesicle
323 release.

324

325 ***iv) Changes in the distribution of multivesicular events***

326 Previous studies quantifying the synaptic transfer of visual information have been
327 limited by the inability to monitor individual active zones and used the assumption that
328 vesicles are released according to Poisson statistics[34,35]. But we now know that bipolar
329 cells do not employ a simple rate-code and visual information is also contained in the
330 *amplitude* of multivesicular events[17]. We therefore tested whether modulation of
331 contrast gain was accompanied by changes in Q_e, the number of quanta in an event.

332 A comparison of the distribution of Qe in the morning and afternoon is shown in
333 Fig. 7 for responses to a stimulus of 60% contrast. In ON synapses, 68% of release
334 events in the morning were univesicular, falling to 40% in the afternoon and reflecting
335 a shift in the distribution towards larger events (Fig. 7B; $p < 0.05$, KS test). This shift
336 towards MVR was fully reversed by antagonizing D1 receptors by injection of SCH

337 23390 (Fig. 7C). In the morning, MVR was more prevalent in OFF synapses with only
338 38% of release events being univesicular but again there was a significant shift
339 towards larger events in the afternoon (Fig. 7D; $p<0.02$). Blocking the D1 actions of
340 endogenous dopamine had a stronger effect in OFF synapses, increasing the
341 proportion of univesicular events to 66% in the afternoon (Fig. 7E; $p < 0.001$).
342 Qualitatively similar modulation of MVR was observed over a range of contrasts from
343 20% to 80% and blocking D1 receptors in the afternoon shifted the distribution back to
344 univesicular release in both ON and OFF channels (Fig. 7D and E). Diurnal variations
345 in dopamine therefore modulate MVR.

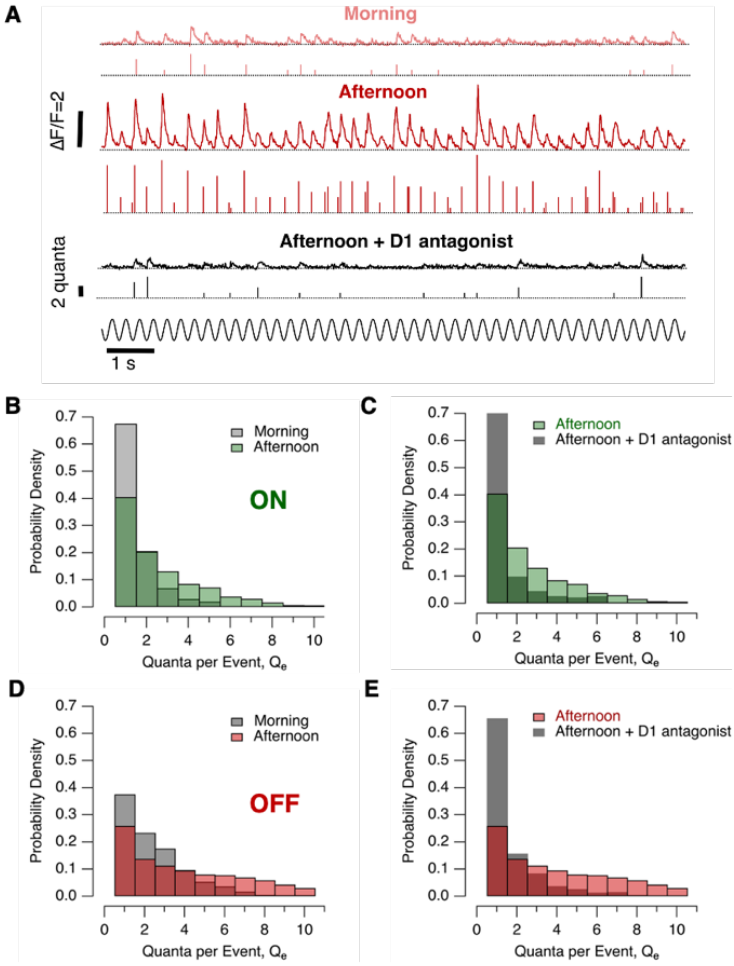

346

347 **Figure 7. Dopamine contributes to diurnal variations in the distribution of multivesicular events**
348 A. Examples of iGluSnFR signals from individual synapses elicited using 60% contrast stimulus (5 Hz,
349 30 sec) in the morning (top), afternoon (middle) and afternoon + SCH 23390 (bottom). In each case the top
350 trace shows the iGluSnFR signal and the lower trace the estimated Q_e. **B**. Changes in Q_e in ON synapses
351 in the morning and afternoon. In the afternoon the distribution was shifted toward multiquantal events

352 (p<0.059, Chi-squared test). **C.** Changes in the distribution of Q_e in ON synapses before and after
353 intravitreal injection of the D1 antagonist SCH23390. The distribution was shifted toward lower Q_e
354 (p<0.001) but was not significantly different to that measured in the morning. **D.** Changes in Q_e, in OFF
355 synapses in the morning and afternoon. In the afternoon the distribution was shifted toward multiquantal
356 events (p<0.007). **E.** Changes in the distribution of Q_e in OFF synapses before and after intravitreal
357 injection of SCH 23390 in the afternoon. The distribution was shifted toward uniquantal events (p<0.001).
358

359 **Modulation of information encoded at the synapse**

360 How do changes in synaptic gain (Figs. 2-3), noise (Fig. 4-6) and MVR (Fig. 7)
361 combine to alter the amount of visual information transmitted by the synapses of
362 bipolar cells? A larger synaptic signal relative to noise (SNR) will tend to increase the
363 mutual information (I) between the response (q) and the stimulus generating it (S),
364 although the size of the increase will depend on the statistical properties of both signal
365 and noise[36]. In the simple situation where both have a Gaussian distribution I =
366 $0.5\log_2(1+SNR)$. But how should we quantify the synaptic signal? When analyzing the
367 spike code, all events comprise the same symbol and the response can be described
368 as the number of spikes in each of a series of time bins[22,36]. The output from bipolar
369 cells is qualitatively different with a visual stimulus being encoded both by the timing of
370 release events and their amplitudes[17]. We therefore took an approach in which MVR
371 composed of different numbers of vesicles were considered different symbols[21,37]. The
372 mutual information between the response and stimulus was then computed as the
373 average amount of information about the stimulus gained from observing any symbol
374 (see Methods).

375 The stimulus set S comprised 12 different contrasts but these were not fixed for
376 each synapse because the contrast sensitivity varied between synapses and between
377 morning and afternoon (Fig. 1E-G). To make allowance for this, we used contrasts
378 spanning ±10% around $C_{1/2}$ measured within the synapse under study immediately
379 before delivering the stimulus set. In the absence of information about the distribution
380 of contrasts normally experienced by a larval zebrafish, a uniform distribution of

contrasts was used for S. Each contrast step lasted 2 s (5 Hz) and they were presented in two different pseudo-random orders, of which one is shown in Fig. 8A.

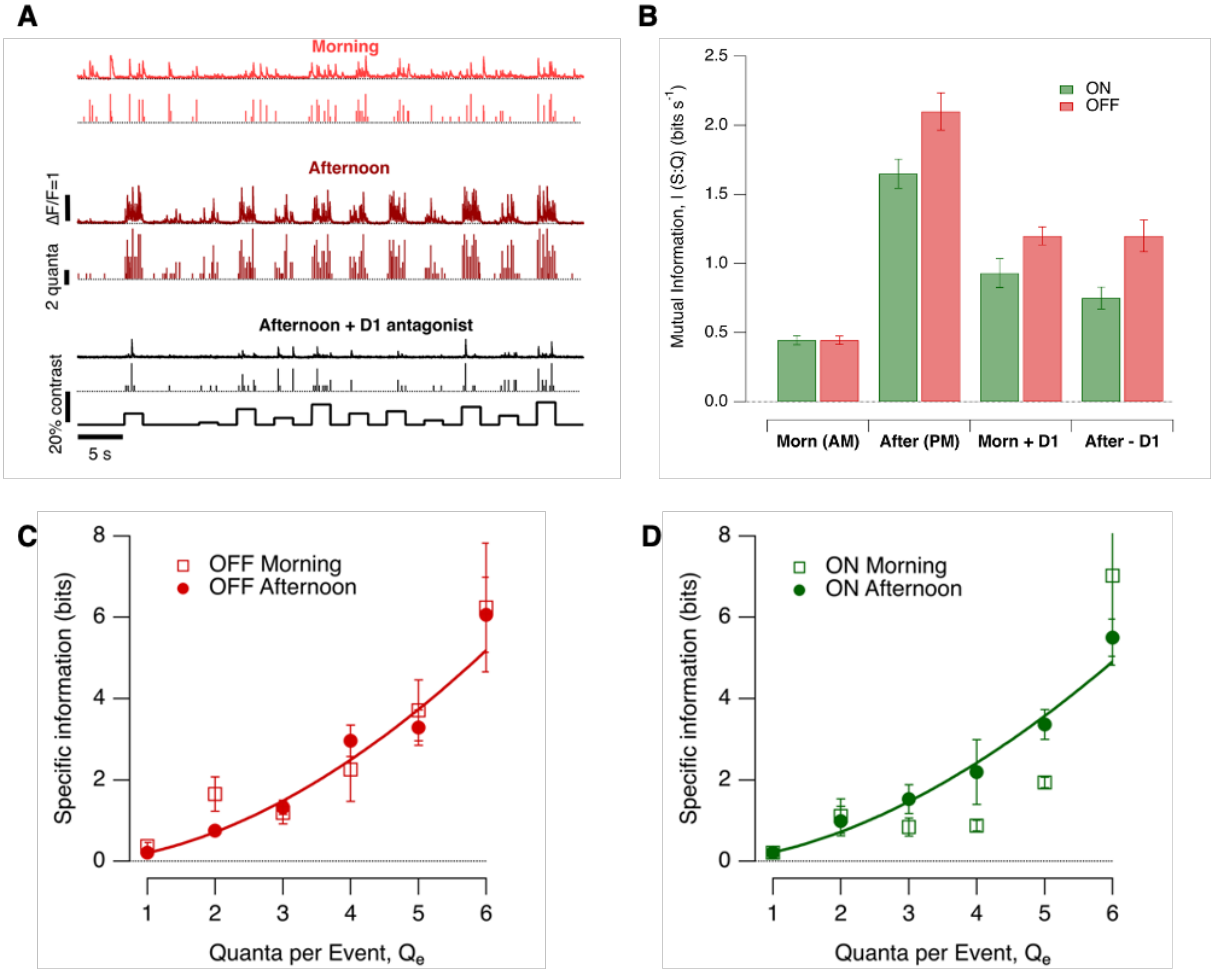

Figure 8. Diurnal changes in the efficiency with which synapses transmit visual information

A. Examples of synaptic responses over 12 different contrasts spanning ±10% around the contrast eliciting the half-maximal response ($C_{1/2}$) in the morning (top, light red), afternoon (middle, dark red) and after injection of D1 antagonist SCH 23390 in the afternoon (bottom, black; note the lower frequency and amplitude of release events). In each case the top trace shows the iGluSnFR signal and the lower trace the estimated Q_e. Each contrast step lasted 2 s (5 Hz) and each trace is from a different OFF synapse. **B.** Mutual information *I (S;Q)* in four conditions: (i) morning, (ii) afternoon, iii) morning after injection of ADTN, (iv) afternoon after injection of SCH 23390. **C.** Specific information (I_2) for events of different quantal content in OFF synapses (33 synapses). The curve describing the relation is a least-squares fit of a power function of the form $i = AQ_e^x$, with A = 0.20, and x = 1.81. **D.** As C, but for ON synapses (n = 13). The curve describing the relation is almost identical (A = 0.21, and x = 1.75).

396 In the morning, the average mutual information between stimulus and response
397 was almost exactly the same for synapses in the ON and OFF channels (0.445 ±
398 0.035 bits s^{-1} and 0.455 ± 0.03 bits s^{-1}, respectively). In the afternoon mutual
399 information increased through both channels although the increase in OFF synapses
400 (370%) was significantly larger than in ON (270%; $p < 0.001$; Fig. 8B). In OFF
401 synapses, the maximum mutual information of 2.1 bits s^{-1} was associated with average
402 release rate of 2.5 vesicles s^{-1} around $C_{1/2}$, equivalent to an efficiency around 0.8 bits
403 per vesicle.

404 Several of the synaptic properties we have analyzed will contribute to the
405 improvement in information transmission in the afternoon, including the increase in
406 synaptic gain (Fig. 2), the decrease in spontaneous noise (Fig. 3) and reduced
407 variability of stimulus-evoked responses (Figs. 5 and 6). These aspects of synaptic
408 transmission were all subject to modulation by dopamine and, consistent with these
409 changes, mutual information in the morning was increased by activation of D1
410 receptors while in the afternoon it was decreased by antagonizing the effects of
411 endogenous dopamine (Fig. 8B).

412 These results demonstrate that information transmission through the retina is
413 under diurnal control and that dopamine is a key neuromodulator controlling these
414 changes. Antagonizing D1 receptors did not, however, reduce mutual information to
415 levels measured in the morning, leaving open the possibility that other signaling
416 pathways also contribute.

417

418 **Changes in the efficiency of the vesicle code**

419 The transmission of information using spikes and vesicles is the major consumer of
420 energy in the brain with one estimate being of the order of ~24,000 ATP molecules per
421 bit[38,39]. The largest part of this energy consumption is taken up by synaptic
422 transmission so a key question becomes the effect of neuromodulation on the
423 efficiency with which vesicles are used to transmit information. Strikingly, the 2.7-fold

424 increase in information transmitted through ON synapses in the afternoon (Fig. 8B)
425 was *not* associated with any change in the average rate of vesicle release (Fig. 2D and
426 E), while the 3.7-fold increase in OFF synapses was associated with only a 2-fold
427 increase in the rate around $C_{1/2}$ (Fig. 2C and E). The diurnal increase in synaptic gain
428 was therefore associated with a 1.4- to 2.7-fold increase in the average efficiency with
429 which vesicles were used to encode changes in contrast. A comparison can be made
430 with the information transmitted by spikes in RGCs, where the most sluggish cells
431 transmit ~3.5 bits/spike, while those that fire most briskly encode ~2 bits/spike[40]. An
432 increase in spike rate is therefore associated with a *decrease* in the visual information
433 per spike while an increase in vesicle release rate is associated with an i*ncrease* in
434 information per vesicle.

435 How is this increase in the efficiency of the vesicle code achieved? The
436 comparison of information transmission with average rates of vesicle release obscures
437 a key aspect of the vesicle code operating in bipolar cells: information about contrast is
438 represented as changes in both the rate and amplitude of release events[23]. This is
439 significant because the distribution of MVR events was also a function of *Zeitgeber*
440 time and larger events are rarer and carry more specific information[17], as shown by the
441 supralinear relation between the specific information carried by each synaptic symbol
442 and the number of vesicles it contains (Fig. 8C-D). The diurnal modulation of the
443 efficiency of the vesicle code therefore depends on the shift between univesicular and
444 multivesicular release (Fig. 7B and D).

445 We also considered the possibility that modulation of retinal processing might be
446 accompanied by changes in the amount of information carried by a given synaptic
447 symbol. The relation between information carried and event amplitude did not,
448 however, change in the afternoon compared to the morning, at least for events
449 composed of 1-6 vesicles (Fig. 8C-D; OFF synapses $p>0.99$; ON synapses $p>0.98$; KS
450 test).

451

452 **Discussion**

453 The plasticity of synapses allows the flow of information through circuits to be
454 modulated[1] and this study provides a quantitative understanding of this idea in the
455 context of the diurnal control of visual processing in the retina. We find that the daily
456 light-dark cycle alters the transmission of visual information through bipolar cells by
457 factors of ~4 during daylight hours by adjusting four synaptic properties; the number of
458 vesicles released by a stimulus (Fig. 3), spontaneous synaptic noise (Fig. 4), the
459 variability of stimulus-driven responses (Figs. 5-6) and the balance between
460 univesicular and multivesicular release (Fig. 7). Crucially, the switch in emphasis from
461 univesicular to multivesicular release also increases the amount of information
462 transmitted per vesicle (Fig. 8). Dopamine plays a major role in regulating all these
463 aspects of retinal function although the relative contributions of these mechanisms
464 differed between ON and OFF pathways.

465

466 **Diurnal modulation of gain**

467 Dopamine-dependent changes in the synaptic gain of bipolar cells might be caused
468 either by direct modulation of processes within the terminal compartment or by actions
469 on the circuitry in which they are embedded. A direct action is strongly supported by
470 the presence of dopamine receptors (especially D1) on the terminal compartment of
471 bipolar cells[41,42] and electrophysiological experiments demonstrating that their
472 activation potentiates L-type calcium channels that control vesicle fusion[4]. Dopamine
473 also acts on D2 receptors on cone synapses to potentiate the visual drive to bipolar
474 cells but this mechanism alone does not easily explain the *transient* increase in
475 contrast-sensitivity in the afternoon given that luminance sensitivity, a much more
476 direct reflection of the strength of cone input, gradually increases throughout the day
477 (cf. Fig. 1B and Fig. 1E). The gain of bipolar cell synapses is also strongly dependent
478 on the inhibitory inputs that the synaptic compartments receives from amacrine cells
479 and the possibility of diurnal modulation of inhibition remains open.

480 Dopamine release is controlled by the internal circadian clock as well as changes
481 in luminance[7] or the appearance of food-related odours[4]. But other neuromodulators,
482 are also released from amacrine cells, including melatonin[43], Substance P[44] and
483 somatostatin[45] and some of these can antagonize the actions of others[44]. A large
484 number of different proteins control the activity of the retinal circuit and 17% of genes
485 in zebrafish are under circadian regulation[7]. There is therefore a good possibility that
486 neuromodulators other than dopamine will also act on the synaptic output of bipolar
487 cells, either directly or indirectly, to regulate the visual signal transmitted to ganglion
488 cells.
489
490 **Diurnal modulation of noise**
491 It has long been appreciated that synaptic noise can reduce the amount of information
492 transmitted through a circuit of neurons[28]. When the retina operates under photopic
493 conditions, for instance, the release of vesicles from bipolar cells adds noise to the
494 signal arriving from cones and therefore causes a loss of information in RGCs[46]. It has
495 been suggested, however, that under other circumstances the noise in synaptic
496 transmission might improve information transmission, such as when stochastic
497 resonance increases the probability of post-synaptic depolarization crossing threshold
498 for spike generation[29,47]. But it seems unlikely that the retina operates under such a
499 regime, given that diurnal increases in synaptic gain went hand-in-hand with a
500 reduction in several sources of noise, including spontaneous release unrelated to a
501 stimulus.
502 All the changes in synaptic function that we observed comparing periods in the
503 morning and afternoon were mimicked by manipulating dopamine signalling, indicating
504 that this neuromodulator adjusts information transmission by orchestrating changes in
505 both the signal and the various noise sources that cause it to vary. The balance
506 between modulation of signal and noise was however, strikingly different in the ON
507 channel, where synaptic gain was *not* under diurnal modulation, compared to the OFF

508 channel, where both signal and noise were regulated. The processes by which
509 dopamine and other neuromodulators adjust synaptic noise are also likely to involve
510 both direct actions on the synaptic compartment and indirect actions on other
511 components of the retinal circuit.
512
513 **Modulation of multivesicular release**
514 MVR is not just a property of ribbon synapses but is also a feature of synaptic
515 transmission in the hippocampus[48], cerebellum[49] and somatosensory cortex[19], where
516 arrival of a spike can often trigger release of two or more vesicles at an active zone. A
517 recent combination of electrophysiology with correlative light-and electron-microscopy
518 has even led to the suggestion that MVR may be a fundamental mode of synaptic
519 transmission throughout the nervous system[20]. It is also recognized that MVR can be
520 adjusted by neuromodulation, for instance through muscarinic acetylcholine receptors
521 in the striatum{Higley, 2009 #221} or $GABA_B$ receptors in the cortex**{**Chalifoux, 2010
522 #222}, athough the implications for information transmission in these contexts is not
523 known. Our study has demonstrated that potentiation of MVR in the retina not only
524 increases the amount of information that a synapse can transmit using vesicles but
525 also the efficiency of coding. It will be interesting to establish how far neuromodulators
526 acting in other parts of the brain alter the efficiency of the information transmission and
527 how far this involves modulation of MVR as compared to the variability and noise that
528 is a feature of central synapses[28,29]. A crucial aspect of these questions will be to
529 understand how switching from univesicular release to multivesicular release alters the
530 spike code generated post-synaptically.
531
532
533

Acknowledgements

The authors express many thanks to all the members of Lagnado laboratory for discussion. We also thank Tom Baden for his many insightful criticisms and suggestions. This work was supported by grants to L.L. from the Wellcome Trust (102905/Z/13/Z).

Author contributions

J. M-D. conceived, designed and executed experiments, analyzed results and prepared the manuscript. B. J. carried out analysis and wrote code. F. E. conceived and executed experiments and carried out analysis. J. J. conceived and executed experiments and carried out analysis. L. L. conceived the project, designed experiments, analyzed data, repaired equipment, wrote code and prepared the manuscript.

Supplementary Information

Supplementary Figure 1

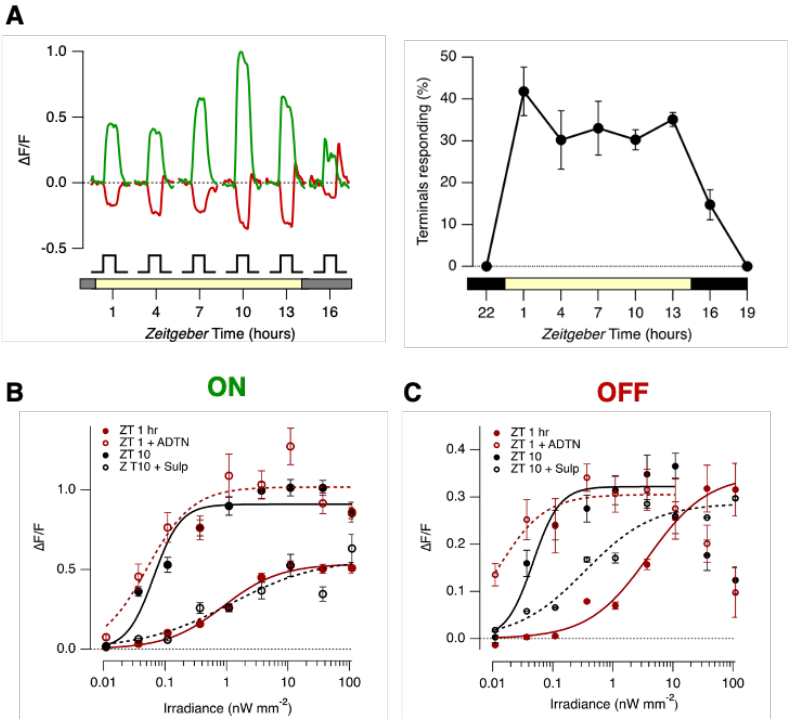

Figure S1. Diurnal changes in luminance sensitivity are co-ordinated by dopamine

A. Left: Averaged SyGaMP2 signals at different *Zeitgeber* time. ON terminals green and OFF terminals red. Each step of light (10 nW mm^{-2}) lasted 3 s. These averages are only from responsive terminals. Right: the percentage of terminals generating a significant response to the same light step (averaged across both ON and OFF). Bars show SD. **B.** Effects of manipulating dopamine signalling on luminance sensitivity of the ON channel. Luminance vs. response plots for ON terminals. Red circles compare this function at ZT 1 hr under control conditions (solid circle) and after injection of the non-selective dopamine receptor agonist ADTN (~0.2 μM; open circles). ADTN caused a prompt change in the luminance-response function to forms measured at ZT 10 hrs (solid black circles), increasing R_{max} from 0.53 ± 0.02 to 1.02 ± 0.07, and reducing $I_{1/2}$ from 0.88 ± 0.18 nW mm^{-2} to 0.05 ± 0.02 nW mm^{-2} (± sd, as estimated from the fitted Hill function shown). The higher gain and luminance sensitivity at ZT 10 hrs could be explained as an effect of dopamine at D2 receptors, because it was completely reversed by injection of the selective D2 receptor antagonist sulpiride (~2 μM; open black circles; R_{max} = 0.57 ± 0.13, $I_{1/2}$ = 1.16 ± 1.34 nW mm^{-2}). Results collected from *n* = 535 terminals from 38 fish. **C.** Effects of manipulating dopamine signalling on luminance sensitivity of the OFF channel. Comparing control responses at ZT 1 hr and 10 hrs showed a significant reduction in $I_{1/2}$ from 3.9 ± 1.3 to 0.0128 ± 0.005, but *without* a significant change in R_{max} (0.35 ± 0.03 vs 0.30 ± 0.02). ADTN injected at ZT 1 caused a prompt increase in luminance sensitivity, reducing $I_{1/2}$ to 0.013 ± 0.005 nW mm^{-2}. The higher luminance sensitivity at ZT 10 hrs could be partly explained as an effect of dopamine at D2 receptors, because injection of sulpiride (~2 μM; open black circles) increased $I_{1/2}$ from 0.05 ± 0.01 nW mm^{-2} to 0.35 ± 0.14 nW mm^{-2}. Results collected from *n* = 355 terminals from 38 fish.

572 **Supplementary Figure 2**

573

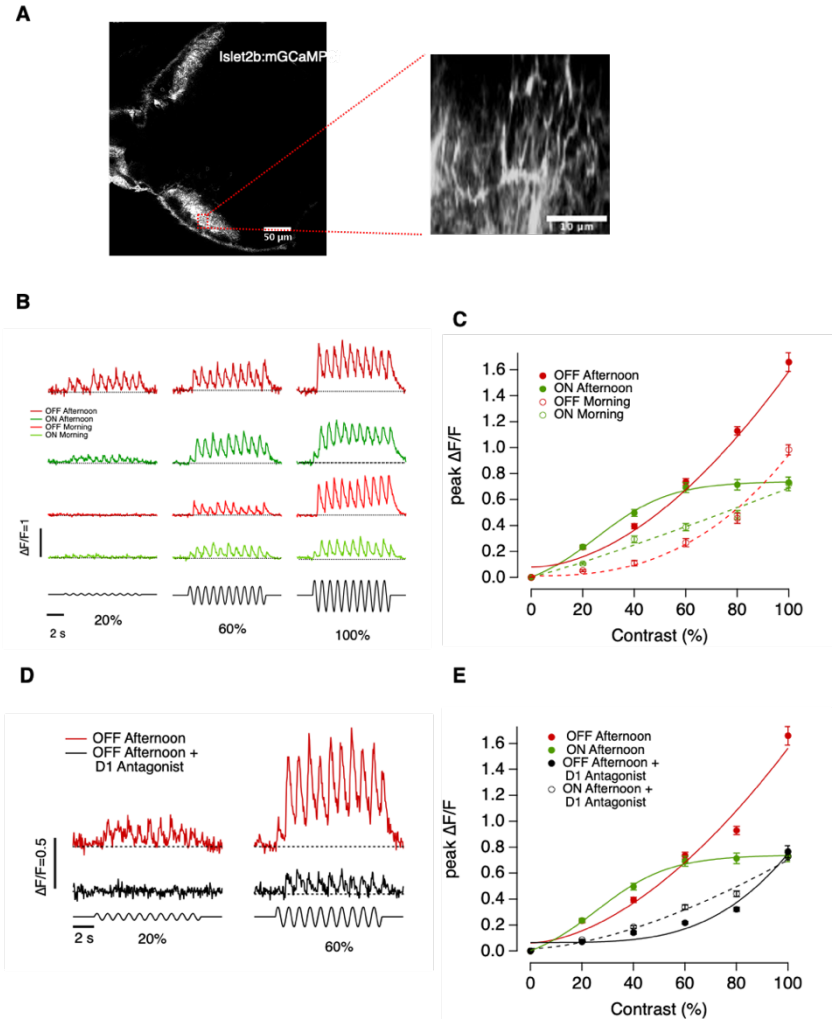

574

575 **Figure S2: Diurnal changes in the visual signal delivered to the optic tectum**

576 **A.***Left panel*. Multiphoton section through the tectum of a zebrafish larva islet2b::mGCaMP6f (7 dpf)
577 expressing the calcium reporter mGCaMP6f, which labels axons and synaptic terminals of retinal ganglion
578 cells (RGCs). *Right panel*. Blow-up of the square red shown in the left panel. The image shows the Z
579 plane reconstruction from where the synaptic responses were recorded. **B.** mGCaMP6f signals from
580 individual ON and OFF RGCs synapses elicited using a stimulus contrasts of 20%,60% and 100 %
581 modulated at 1 Hz (full field, sine wave) **C.** Average contrast-response functions displayed by ON and
582 OFF RGCs, where the response (*R*) was quantified as the average of the fluorescence peak amplitudes
583 measured at each cycle of stimulation. Each point shows the mean ± s.e.m. Note the differences in the
584 magnitude of the responses between OFF RGCs in the morning relative to afternoon. **D.** mGCaMP6f
585 signals from an individual OFF RGCs before and after intravitreal injection of the D1 antagonist in the
586 afternoon. **E.** Average contrast-response function displayed by ON and OFF RGCs before and after
587 administration of the D1 antagonist in the afternoon. Note the dramatic decrease in the magnitude of the
588 response in both ON and OFF channels.

589

590 **Supplementary Figure 3**
591
592

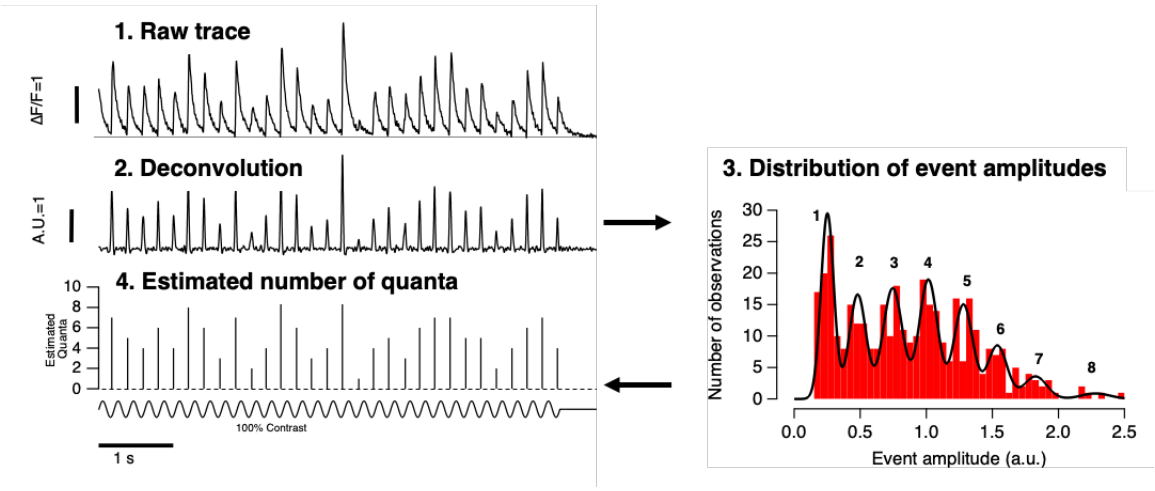

593
594 **Figure S3. Decomposition of iGluSnFR signals into vesicle counts**
595 Summary of the basic steps for quantal decomposition of iGluSnFr signals. *1*. Raw trace extracted from
596 individual active zones (linescan, 1 KHz). *2*. Deconvolved trace using the estimated Wiener filter. *3*.
597 Histogram of event amplitudes for a representative active zone (373 events accumulated using stimulus
598 contrasts of 20%, 60% and 100% and a frequency of 5 Hz). The black line is a fit of eight Gaussians,
599 identified using a Gaussian mixture model. Note that the variance of successive Gaussians did not
600 increase in proportion to the peak number. The first peak had a value of 0.24, and the distance between
601 peaks averaged 0.25, indicating the existence of a quantal event equivalent to ~0.25. ***.4.*** Estimation of the
602 number of quanta per event. For more details about analyses see James et al., 2019.
603

604 # Methods

605

606 **Zebrafish husbandry**

607 Fish were raised and maintained under standard conditions on a 14 h light/10 h dark
608 cycle[35]. To aid imaging, fish were heterozygous or homozygous for the casper mutation
609 which results in hypopigmentation and they were additionally treated with1-phenyl-2-
610 thiourea (200 μM final concentration; Sigma) from 10 hours post fertilization (hpf) to
611 reduce pigmentation. All animal procedures were performed in accordance with the
612 Animal Act 1986 and the UK Home Office guidelines and with the approval of the
613 University of Sussex Animal Welfare and Ethical Review Board. More information about
614 experimental design and reagents is available in the Life Sciences reporting Summary.

615

616 **Transgenic fish**

617 Experiments were carried out using the following transgenic lines of zebrafish:

618 i) *Tg(ribeye:;Zf-SyGCaMP2)* expressing the synaptically-localized fluorescent calcium
619 reporter SyGCaMP 2.0 in retinal bipolar cells under the ribeye-A promoter[24].

620 *ii) Tg(–1.8ctbp2:Gal4VP16_BH)* fish that drive the expression of the transcriptional
621 activator protein Gal4VP16 were generated by co-injection of I-SceI meganuclease and
622 endofree purified plasmid into wild-type zebrafish with a mixed genetic background. A
623 myocardium-specific promoter that drives the expression of mCherry protein was
624 additionally cloned into the plasmid to allow for phenotypical screening of founder fish.

625 *iii) Tg(10xUAS:iGluSnFR_MH)* fish driving the expression of the glutamate sensor
626 iGluSnFR under the regulatory control of the 10 x UAS enhancer elements were
627 generated by co-injection of purified plasmid and tol2 transposase RNA into offspring of
628 AB wildtype fish outcrossed to casper wildtype fish. The sequences for the myocardium-
629 specific promoter driving the expression of enhanced green fluorescent protein (mossy
630 heart) were added to the plasmid to facilitate the screening process.

631 iv) *Tg(–1.8ctbp2:SyGCaMP6)* fish were generated by co-injection of I-SceI
632 meganuclease and endofree purified plasmid into wild-type zebrafish with a mixed
633 genetic background. The GCaMP6f variant was kindly provided by L. Looger (Janelia
634 Farm). This variant holds a T383S mutation in comparison to the commercially available
635 GCaMP6-fast version (Addgene plasmid 40755).
636 v) *Tg(isl2b:nlsTrpR, tUAS:memGCaMP6f)* which drives the expression of
637 memGCaMP6f in the optic tectum was generated by co-injecting pTol2-isl2b-hlsTrpR-pA
638 and pBH-tUAS-memGaMP6f-pA plasmids into single-cell stage eggs. Injected fish were
639 out-crossed with wild-type fish to screen for founders.
640
641 **Multiphoton Imaging *In Vivo***
642 Experiments were carried out in a total of 117 zebrafish larvae (7–9 days post-
643 fertilization). Fish were immobilized in 3% low melting point agarose (Biogene) in E2
644 medium on a glass coverslip (0 thickness) and mounted in a chamber where they were
645 superfused with E2. Imaging was carried out using a two-photon microscope (Scientifica)
646 equipped with a mode-locked titanium-sapphire laser (Chameleon, Coherent) tuned to
647 915 nm and an Olympus XLUMPlanFI 20x water immersion objective (NA 0.95). To
648 prevent eye movements, the ocular muscles were paralyzed by injection of 1 nL of α-
649 bungarotoxin (2 mg/mL) behind the eye. Most imaging was carried out in the dorsal the
650 retina.
651 The signal-to-noise ratio of the microscope was optimized by collecting photons
652 through both the objective and a sub-stage oil condenser (Olympus, NA 1.4). Emission
653 was filtered through GFP filters (HQ 535/50, Chroma Technology) before detection with
654 GaAsP photomultipliers (H7422P-40, Hamamatsu). The signal from each detector passed
655 through a current-to-voltage converter and then the two signals were added by a
656 summing amplifier before digitization. Scanning and image acquisition were controlled
657 under ScanImage v.3.6 software[52]. In iGluSnFR recordings images were acquired at
658 10 Hz (128 × 100 pixels per frame, 1 ms per line) while linescans were acquired at 1 kHz.

659 In GCaMP recordings images were acquired at 20 Hz (128 × 50 pixels per frame, 1 ms
660 per line). Full-field light stimuli were generated by an amber LED (l_{max} = 590 nm,
661 Thorlabs), filtered through a 590/10 nm BP filter (Thorlabs), and delivered through a light
662 guide placed close to the eye of the fish. These wavelengths will most effectively
663 stimulate red and green cones. The microscope was synchronized to visual stimulation.
664

665 **Stimulation protocols**

666 Measurements of contrast sensitivity with SyGCaMP2 were made by stimulating the fish
667 with a series of 10 s stimuli (full-field sinusoidal modulation at 5 Hz) around a mean
668 intensity of 55 nW $mm^{-2.}$ Measurements of contrast sensitivity with iGluSnFR used 2 s
669 stimuli. To measure the distribution of events amplitudes and the temporal precision fish
670 were continuously stimulated for 30 s at a given contrast.
671 Luminance sensitivity was assessed by stimulating the fish with a series of light steps
672 (4 x 3 s) at 9 different light intensities increasing in steps of 0.5 log unit steps ranging from
673 11 pW mm^{-2} to 110 nW mm^{-2} (equivalent to 3.3 x 10^{11} photons mm^{-2}).
674

675 **Drug injections**

676 Dopamine signalling was manipulated by injecting the antagonist of D1 receptors SCH
677 23390 at a final estimated concentration of 200 nM (Sigma).Finally, the long-lasting
678 dopamine receptor ligand [3H] 2-amino-6,7-dihydroxy 1,2,3,4-tetrahydronapthalene
679 (ADTN) (Sigma) was injected to a final estimated concentration of 200 nM. We confirmed
680 that these drugs gained access by including 1 mM Alexa 594 in the injection needle;
681 within 5 mins of injection the dye could be detected within the inner plexiform layer of the
682 retina. Vehicle injection did not affect synaptic responses to varying contrast.
683

684 **Calculation of temporal jitter**

685 In order to quantify variability in the timing of glutamatergic events, we first calculated the
686 vector strength, r_q, for events composed of q quanta:

687 $$r_q = \frac{1}{N_q}\sqrt{\left(\sum_{i=1}^{N_q} cos\left(\frac{2\pi t_{q_i}}{T}\right)\right)^2 + \left(\sum_{i=1}^{N_q} sin\left(\frac{2\pi t_{q_i}}{T}\right)\right)^2} \quad (1)$$

688 where t_{qi} is the time of the ith q-quantal event, T is the stimulus period, and N_q is the total
689 number of events of composed of q-quanta. The temporal jitter, J_q, can then be calculated
690 as:

691 $$J_q = \frac{\sqrt{2(1 - r_q)}}{2\pi f} \quad (2)$$

692 where f is the stimulus frequency.

693

694 **Calculations based on Information Theory**

695 To quantify the amount of information about a visual stimulus that is contained within
696 the sequence of release events from an active zone we first needed to convert bipolar
697 cell outputs into a probabilistic framework from which we could evaluate the specific
698 information (I_2), a metric that quantifies how much information about one random
699 variable is conveyed by the observation a specific symbol of another random
700 variable[36]. The time series of quantal events was converted into a probability
701 distribution by dividing into time bins of 20 ms, such that each bin contained either zero
702 events or one event of an integer amplitude. We then counted the number of bins
703 containing events of amplitude 1, or 2, or 3 etc. By dividing the number of bins of each
704 type by the total number of bins for each different stimulus, we obtained the conditional
705 distribution of **Q** given **S**, $p(\boldsymbol{Q}|\boldsymbol{S})$, where **Q** is the random variable representing the
706 *quanta/bin* and **S** is the random variable representing the *stimulus contrasts* presented
707 throughout the course of the experiment. In the absence of information about the
708 distribution of contrasts normally experienced by a larval zebrafish, a uniform

distribution of contrasts was used for S. Each contrast step lasted 2 s (5 Hz) and they were presented in two different pseudo-random orders, of which one is shown in Fig. 4D. The contrast sensitivity varied between synapses and between morning and afternoon (Fig. 1E-G) so to make allowance for this the stimulus set S was adjusted for each synapse to span contrasts ±10% around $C_{1/2}$ measured within that synapse.

We computed the joint probability distribution by the chain rule for probability (given the experimentally defined uniform distribution of stimuli **S**):

$$\boldsymbol{p(S,Q) = p(Q|S)p(S)} \tag{7}$$

In order to convert this distribution into the conditional distribution of S given Q, we used the definition of the conditional distribution:

$$\boldsymbol{p(S|Q) = \frac{p(S,Q)}{p(Q)}} \tag{8}$$

From these distributions we computed two metrics: the mutual information I(**S;Q**)[53] and specific information I_2(**S;q**)[37]. Mutual information is defined traditionally as:

$$\mathbf{I}(\boldsymbol{S;Q}) = \boldsymbol{H(S) - H(S|Q)} \tag{9}$$

$$\mathbf{I}(\boldsymbol{S;Q}) = \sum_{s\in S}\sum_{q\in Q} \boldsymbol{p(s,q)}\,\mathbf{log_2}\,\boldsymbol{\frac{p(s)p(q)}{p(s,q)} = I(Q;S)} \tag{10}$$

The specific information, I_2(**S;q**), is defined as the difference between the entropy of the stimulus S minus the conditional entropy of the stimulus given the observed symbol in the response q:

$$\boldsymbol{I_2(S,q) = H(S) - H(S|q)} \tag{11}$$

$$\boldsymbol{I_2(S,q) = -\sum_{s\in S} p(s)\,log\,p(s) + \sum_{s\in S} p(s|q)\,log\,p(s|q)} \tag{12}$$

representing the amount of information observing each quantal event type q ϵ **Q** carries about the stimulus distribution **S**. Note that mutual information can also be computed from the specific information as the dot product of the specific information vector $\boldsymbol{I_2}$ and the vector describing the probability of an event of a given quantal size $\boldsymbol{p(q)}$. This adds to the interpretability of both metrics – the specific information is the amount of information a

single (specific) symbol gives about the stimulus, and the mutual information is the average amount of information about the stimulus gained from observing any symbol.

Measuring entropy and mutual information from neural responses can be a challenging problem. Estimates require sampling from an unknown discrete probability distribution, and in many cases recording sufficient samples to observe all non-zero probability events is neither tractable nor practical. The biases introduced by undersampling can be a particular problem when the full support of the distribution (all values that map to non-zero probabilities) is high. Within the past few decades, various approaches to correcting biases in information theoretic analyses have been developed[54]. However, as the distributions of interest in this work have both a small support and are well sampled, we have opted to use standard estimates for the quantities of interest.

Statistics

All data are given as mean ± s.e.m. unless otherwise stated in the figure legends. All statistical tests met appropriate assumptions and were calculated using inbuilt functions in IgorPro (Wavemetrics). When data were not normally distributed we used non-parametric tests. Significance was defined as $p < 0.05$. Data collection was not randomized because all experiments were carried out within one set of animals. Delivery of different stimuli was randomized where appropriate. Data were only excluded from the analysis if the signal-to-noise ratio (SNR) of the iGluSnFR signals elicited at a given synapse was not sufficient to detect unitary responses to visual stimuli with a SNR of at least three.

References

1 Bargmann, C. I. & Marder, E. From the connectome to brain function. *Nat Methods* **10**, 483-490, doi:nmeth.2451 [pii]

10.1038/nmeth.2451 (2013).

2 Kastner, D. B. & Baccus, S. A. Coordinated dynamic encoding in the retina using opposing forms of plasticity. *Nature neuroscience* **14**, 1317 (2011).

3 Johnston, J. *et al.* A Retinal Circuit Generating a Dynamic Predictive Code for Oriented Features. *Neuron* **102**, 1211-1222 e1213, doi:10.1016/j.neuron.2019.04.002 (2019).

4 Esposti, F., Johnston, J., Rosa, J. M., Leung, K. M. & Lagnado, L. Olfactory stimulation selectively modulates the OFF pathway in the retina of zebrafish. *Neuron* **79**, 97-110, doi:10.1016/j.neuron.2013.05.001 (2013).

5 Schroder, S. *et al.* Arousal Modulates Retinal Output. *Neuron* **107**, 487-495 e489, doi:10.1016/j.neuron.2020.04.026 (2020).

6 Ribelayga, C., Cao, Y. & Mangel, S. C. The circadian clock in the retina controls rod-cone coupling. *Neuron* **59**, 790-801, doi:10.1016/j.neuron.2008.07.017 (2008).

7 Li, L. Circadian Vision in Zebrafish: From Molecule to Cell and from Neural Network to Behavior. *J Biol Rhythms* **34**, 451-462, doi:10.1177/0748730419863917 (2019).

8 Zang, J. *et al.* Circadian regulation of vertebrate cone photoreceptor function. *eLife* **10**, e68903, doi:10.7554/eLife.68903 (2021).

9 Jackson, C. R. *et al.* Retinal dopamine mediates multiple dimensions of light-adapted vision. *The Journal of neuroscience : the official journal of the Society for Neuroscience* **32**, 9359-9368, doi:10.1523/JNEUROSCI.0711-12.2012 (2012).

10 Euler, T., Haverkamp, S., Schubert, T. & Baden, T. Retinal bipolar cells: elementary building blocks of vision. *Nat Rev Neurosci* **15**, 507-519, doi:10.1038/nrn3783 (2014).

11 Nikolaev, A., Leung, K. M., Odermatt, B. & Lagnado, L. Synaptic mechanisms of adaptation and sensitization in the retina. *Nat Neurosci* **16**, 934-941, doi:10.1038/nn.3408 (2013).

12 Zimmermann, M. J. Y. *et al.* Zebrafish Differentially Process Color across Visual Space to Match Natural Scenes. *Curr Biol* **28**, 2018-2032.e2015, doi:10.1016/j.cub.2018.04.075 (2018).

13 Matsumoto, A. *et al.* Direction selectivity in retinal bipolar cell axon terminals. *Neuron* (2021).

14 Lagnado, L. & Schmitz, F. Ribbon Synapses and Visual Processing in the Retina. *Annu Rev Vis Sci* **1**, 235-262, doi:10.1146/annurev-vision-082114-035709 (2015).

15 Glowatzki, E. & Fuchs, P. A. Transmitter release at the hair cell ribbon synapse. *Nat Neurosci* **5**, 147-154, doi:10.1038/nn796 (2002).

16 Singer, J. H., Lassova, L., Vardi, N. & Diamond, J. S. Coordinated multivesicular release at a mammalian ribbon synapse. *Nat Neurosci* **7**, 826-833, doi:10.1038/nn1280 (2004).

17 James, B., Darnet, L., Moya-Diaz, J., Seibel, S. H. & Lagnado, L. An amplitude code transmits information at a visual synapse. *Nat Neurosci* **22**, 1140-1147, doi:10.1038/s41593-019-0403-6 (2019).

18 Lisman, J. E., Raghavachari, S. & Tsien, R. W. The sequence of events that underlie quantal transmission at central glutamatergic synapses. *Nat Rev Neurosci* **8**, 597-609, doi:10.1038/nrn2191 (2007).

19 Huang, C.-H., Bao, J. & Sakaba, T. Multivesicular Release Differentiates the Reliability of Synaptic Transmission between the Visual Cortex and the Somatosensory Cortex. *The Journal of Neuroscience* **30**, 11994, doi:10.1523/JNEUROSCI.2381-10.2010 (2010).

20 Holler, S., Köstinger, G., Martin, K. A. C., Schuhknecht, G. F. P. & Stratford, K. J. Structure and function of a neocortical synapse. *Nature* **591**, 111-116, doi:10.1038/s41586-020-03134-2 (2021).

21 Shannon, C. A Mathematical Theory of Communication. *Bell System Technical Journal* **27**, 379-423 (1948).

22 Borst, A. & Theunissen, F. E. Information theory and neural coding. *Nat Neurosci* **2**, 947-957, doi:10.1038/14731 (1999).

23 Marvin, J. S. *et al.* An optimized fluorescent probe for visualizing glutamate neurotransmission. *Nat Methods* **10**, 162-170, doi:10.1038/nmeth.2333 (2013).

24 Dreosti, E., Odermatt, B., Dorostkar, M. M. & Lagnado, L. A genetically encoded reporter of synaptic activity in vivo. *Nat Methods* **6**, 883-889, doi:10.1038/nmeth.1399 (2009).

25 Emran, F., Rihel, J., Adolph, A. R. & Dowling, J. E. Zebrafish larvae lose vision at night. *Proceedings of the National Academy of Sciences* **107**, 6034, doi:10.1073/pnas.0914718107 (2010).

26 Nie, K. *et al.* Effects of circadian clock protein Per1b on zebrafish visual functions. *Chronobiology international* **35**, 160-168 (2018).

27 Ashmore, J. & Copenhagen, D. An analysis of transmission from cones to hyperpolarizing bipolar cells in the retina of the turtle. *The Journal of Physiology* **340**, 569-597 (1983).

28 Faisal, A. A., Selen, L. P. & Wolpert, D. M. Noise in the nervous system. *Nat Rev Neurosci* **9**, 292-303, doi:10.1038/nrn2258 (2008).

29 Rusakov, D. A., Savtchenko, L. P. & Latham, P. E. Noisy Synaptic Conductance: Bug or a Feature? *Trends Neurosci* **43**, 363-372, doi:10.1016/j.tins.2020.03.009 (2020).

30 Berry, M. J., Warland, D. K. & Meister, M. The structure and precision of retinal spike trains. *Proceedings of the National Academy of Sciences* **94**, 5411, doi:10.1073/pnas.94.10.5411 (1997).

31 Churchland, M. M. *et al.* Stimulus onset quenches neural variability: a widespread cortical phenomenon. *Nature Neuroscience* **13**, 369-378, doi:10.1038/nn.2501 (2010).

32 Rathbun, D. L., Warland, D. K. & Usrey, W. M. Spike timing and information transmission at retinogeniculate synapses. *Journal of Neuroscience* **30**, 13558-13566 (2010).

33 Cui, Y., Wang, Y. V., Park, S. J. H., Demb, J. B. & Butts, D. A. Divisive suppression explains high-precision firing and contrast adaptation in retinal ganglion cells. *eLife* **5**, e19460, doi:10.7554/eLife.19460 (2016).

34 Freed, M. A. Quantal encoding of information in a retinal ganglion cell. *J Neurophysiol* **94**, 1048-1056, doi:10.1152/jn.01276.2004 (2005).

35 Odermatt, B., Nikolaev, A. & Lagnado, L. Encoding of luminance and contrast by linear and nonlinear synapses in the retina. *Neuron* **73**, 758-773, doi:10.1016/j.neuron.2011.12.023 (2012).

36 Stone, J. V. *Principles of Neural Information Theory: Computational Neuroscience and Metabolic Efficiency* (Sebtel Press, 2018).

37 DeWeese, M. R. & Meister, M. How to measure the information gained from one symbol. *Network* **10**, 325-340 (1999).

38 Attwell, D. & Laughlin, S. B. An energy budget for signaling in the grey matter of the brain. *Journal of Cerebral Blood Flow & Metabolism* **21**, 1133-1145 (2001).

39 Harris, Julia J., Jolivet, R. & Attwell, D. Synaptic Energy Use and Supply. *Neuron* **75**, 762-777, doi:https://doi.org/10.1016/j.neuron.2012.08.019 (2012).

40 Koch, K. *et al.* How much the eye tells the brain. *Curr Biol* **16**, 1428-1434, doi:10.1016/j.cub.2006.05.056 (2006).

41 Mora‐Ferrer, C., Yazulla, S., Studholme, K. M. & Haak‐Frendscho, M. Dopamine D1‐receptor immunolocalization in goldfish retina. *Journal of Comparative Neurology* **411**, 705-714 (1999).

42 Farshi, P., Fyk-Kolodziej, B., Krolewski, D. M., Walker, P. D. & Ichinose, T. Dopamine D1 receptor expression is bipolar cell type-specific in the mouse retina. *The Journal of comparative neurology* **524**, 2059-2079, doi:10.1002/cne.23932 (2016).

43 Ribelayga, C., Wang, Y. & Mangel, S. C. A circadian clock in the fish retina regulates dopamine release via activation of melatonin receptors. *The Journal of Physiology* **554**, 467-482, doi:https://doi.org/10.1113/jphysiol.2003.053710 (2004).

44 Moya-Díaz, J., James, B. & Lagnado, L. Modulation of the vesicle code transmitting the visual signal in the retina. *bioRxiv*, 2020.2004.2022.056119, doi:10.1101/2020.04.22.056119 (2020).

45 Thermos, K. Functional mapping of somatostatin receptors in the retina: a review. *Vision Research* **43**, 1805-1815, doi:https://doi.org/10.1016/S0042-6989(03)00169-X (2003).

46 Freed, M. A. & Liang, Z. Synaptic noise is an information bottleneck in the inner retina during dynamic visual stimulation. *The Journal of physiology* **592**, 635-651, doi:10.1113/jphysiol.2013.265744 (2014).

47 McDonnell, M. D. & Ward, L. M. The benefits of noise in neural systems: bridging theory and experiment. *Nature Reviews Neuroscience* **12**, 415-425, doi:10.1038/nrn3061 (2011).

48 Christie, J. M. & Jahr, C. E. Multivesicular release at Schaffer collateral-CA1 hippocampal synapses. *The Journal of neuroscience : the official journal of the Society for Neuroscience* **26**, 210-216, doi:10.1523/JNEUROSCI.4307-05.2006 (2006).

49 Auger, C., Kondo, S. & Marty, A. Multivesicular release at single functional synaptic sites in cerebellar stellate and basket cells. *The Journal of neuroscience : the official journal of the Society for Neuroscience* **18**, 4532-4547 (1998).

50 Higley, M. J., Soler-Llavina, G. J. & Sabatini, B. L. Cholinergic modulation of multivesicular release regulates striatal synaptic potency and integration. *Nature neuroscience* **12**, 1121-1128 (2009).

51 Chalifoux, J. R. & Carter, A. G. GABAB receptors modulate NMDA receptor calcium signals in dendritic spines. *Neuron* **66**, 101-113 (2010).

52 Pologruto, T. A., Sabatini, B. L. & Svoboda, K. ScanImage: flexible software for operating laser scanning microscopes. *Biomed Eng Online* **2**, 13, doi:10.1186/1475-925X-2-13 (2003).

53 de Ruyter van Steveninck, R. R., Lewen, G. D., Strong, S. P., Koberle, R. & Bialek, W. Reproducibility and variability in neural spike trains. *Science* **275**, 1805-1808, doi:10.1126/science.275.5307.1805 (1997).

54 Pola, G., Schultz, S. R, Petersen, R. S & Panzeri, S. in *Neuroscience Databases: A Practical Guide* (Springer, Boston, MA, 2003).